Proceedings of the ASME 28th International Conference on Ocean, Offshore and Arctic Engineering
OMAE2009
May 31 - June 5, 2009, Honolulu, Hawaii

OMAE2009-80146

LARGE SCALE TESTS OF STRAIN CAPACITY OF PIPE SECTIONS WITH CIRCUMFERENTIAL DEFECTS SUBJECTED TO INSTALLATION-INDUCED PLASTIC STRAIN HISTORY

Bård Nyhus
SINTEF Materials
and Chemistry
Trondheim, Norway

Erling Østby
SINTEF Materials
and Chemistry
Trondheim, Norway

Zhiliang Zhang
University of Science and
Technology (NTNU)
Trondheim, Norway

Erlend Olsø
SINTEF Materials
and Chemistry
Trondheim, Norway

Per Arne Røstadsand
StatoilHydro
Oslo, Norway

Pål Are Eikrem
StatoilHydro
Trondheim, Norway

ABSTRACT

Installation of offshore pipelines by reeling introduces plastic pre-straining. The pre-strain history is not homogenous and it will vary around the circumference of the pipe. The pre-strain history will modify the yield and flow properties. Also, the fracture toughness may be influenced by the pre-straining. The result is that the bending strain capacity of pipelines during operation will differ depending on how the bending moment coincides with pipe orientation during installation.

Three full scale tests of 12” x-60 pipes with wall thickness 19.3mm and a 3x100 mm outer surface defect were performed to investigate the effect of pre-strain history. Two pipes were pre-strained in bending to 2% strain in the outer fibre and then straightened to simulate the reeling. The final tests to establish the strain capacity during operation as a function of strain history were performed in four point bending with an internal pressure of 325 bar. The strain capacity for the side of the pipe that ends in tension and the side that ends in compression from pre-straining was 1.7% and 2.6 % respectively. The strain capacity of the third test without pre-straining was 5.7%. The results show that pre-straining will modify the strain capacity and the effect must be taken into account in engineering critical assessment of pipes during operation. The effect of prestraining should be evaluated for all installation methods that involve plastic deformation during installation, and not only reeling.

It is important to note that the notch size in the full scale tests was larger than what would normally be accepted for reeling. In addition the notch was positioned in base material and not in weld metal, which is a more realistic position for a notch. The welds are normally overmatched and this might reduce the effect of prestraining.

INTRODUCTION

Pipelines can be subjected to a range of loading scenarios that can include yielding. The main sources of loading that might cause plastic deformation are cold bending during installation and ground movement, thermal loads and accidental loads during operation.

Plastic deformation will modify the yield and flow properties, and residual stresses will be introduced. Also fracture toughness may be influenced by the plastic deformation. These changes should be accounted for in evaluating subsequent loading scenarios.

In this study, the effect of plastic deformation during reel-lay, see Figure 1, of offshore pipelines was examined via full scale testing. The reel-lay method is a fast, cost-effective alternative to the S-lay and J-lay methods for installation of small to medium size steel offshore pipelines. In addition, the quality of the pipeline is enhanced by welding and inspection under controlled conditions on-shore. Reeling operations, however, will induce plastic strain in the pipelines, see Figure 2.

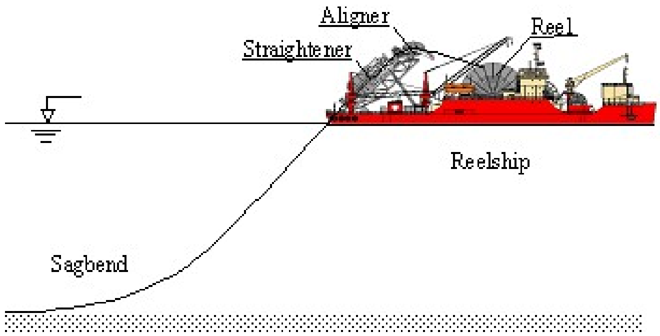

Figure 1 Schematic plot of the pipe reeling process.

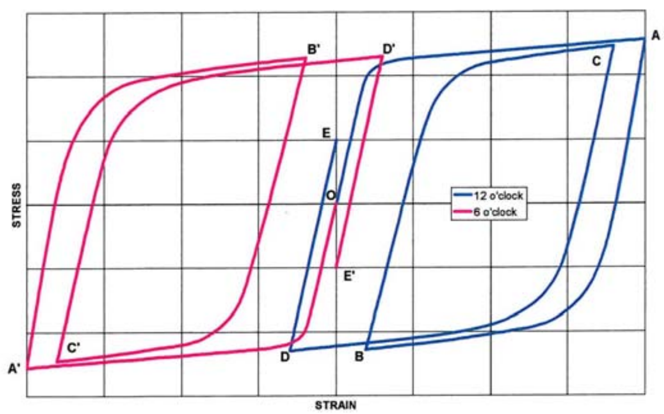

Figure 2 Stresses and strains in the pipe during reel-lay installation (schematic) [1]:

O-A(A'): Reeling-on
A(A')-B(B'): Reeling-off
B(B')-C(C'): Bending over aligner
C(C')-D(D')-E(E'): Through the straightener

DNV-RP-F108 [1] describes how to perform engineering critical assessment (ECA) analyses for reel-lay installation of pipelines, but only installation loads are included in the analyses. It is recommended using a history-independent ductile fracture resistance curve (R-curve). This is based on prior testing that showed that R-curves were not significantly altered by cyclic loading [2-4]. More recent papers, however, conclude that plastic deformation influences, in a detrimental manner, the local failure mechanisms [5-14]. Somewhat in contradiction to DNV-RP-F108, DNV-OS-F101[15] states that for ECA of pipelines that have been subject to plastic strains, fracture mechanics testing shall be performed on pre-strained material. Such testing is to be performed on homogenous pre-strained materials, and the crack is introduced after pre-straining. In real pipelaying operations, cracks due to welding defects may exist before installation. Numerical analyses performed by Eikrem et al.[5] indicate that there will be accumulated ductile damage from the first loading cycle ahead of the crack tip, which will reduce the fracture resistance for the next cycle. This means that the current practice of introducing cracks in the specimens after pre-straining may be unconservative.

The strain capacity of a reel-lay installed pipeline is not only dependent on changes in the fracture toughness. The strain capacity during operation is also dependent on changes in bulk yield and hardening properties due to the plastic deformation during reel-lay. The deformation history will vary around the circumference of the pipeline, and so will the tensile properties after installation. Traditionally, the focus on ECA analyses has been on installation, since axial plastic deformation as large as 2-3% is usually much higher than the deformation during operation. There is, however, increased interest in strain capacity during operation. This is due to potential savings on bottom trenching and rock dumping, which might increase strains during operation. The focus on ECA during operation is also related to the possible effects of pre-strain during installation, as well as the previously demonstrated potential detrimental effect of internal pressure (biaxial stress) on pipe fracture capacity [16].

Pre-straining effects on pipelines are debated and company specific procedures for ECA vary. In the present study, full scale testing of pipes was performed to study the strain capacity after pre-straining. The goal was to find out if installation by reel-lay has a significant effect on the deformation capacity of pipelines with cracks during operation.

PIPE AND DEFECT GEOMETRY

The pipe studied was a 12" seamless X60 steel pipe with nominal outer diameter (OD) of 323.9 mm, and wall thickness, t, of 19.3 mm. Two defects were introduced, by means of sink erosion, in each pipe as shown in Figure 3.The defect size was a=3mm and 2c=100 mm.

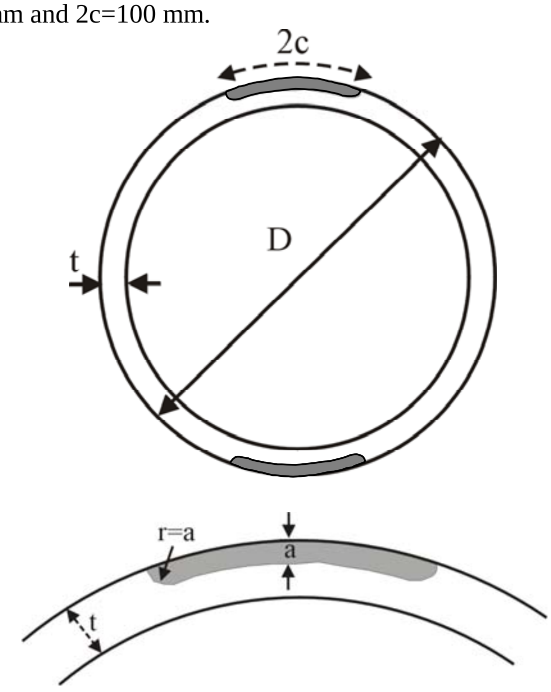

Figure 3 Defect geometry in the pipes.

The cracks were located in base material to cultivate the effect of pre-straining. Testing in a weld zone with inhomogenous material properties can raise questions about crack positioning and uneven strain in the pipes during testing. The test part of the pipe was cut from the same pipe to further reduce the chances for differences in geometry and material properties. The central test part was 4 m. long. This part was elongated by butt welding of a similar pipe in each end to fit the test rigs. Three specimens with the same geometry were prepared for full scale testing.

TEST SETUP

The testing was divided in two parts. The first part was pre-straining to simulate the deformation during a reel-lay installation of the pipe and the second part was testing to establish the bending strain capacity during operation as a function of pre-straining. In addition some small scale tests were performed to establish tensile properties and fracture toughness as a function of pre-straining. All the testing has been performed at room temperature.

Pre-straining Of Full Scale Pipes

Pre-straining of two of the notched pipes was performed at Technip's spoolbase located in Orkanger (Norway). The pipe was first bent over a fixed-radius shoe with the same curvature as the hub diameter of the reel of the Apache pipelay vessel (16.5 m), see Figure 10a. The pipe was then unloaded and the crack on the tension side was examined by silicon replica. The pipes were then reverse bent over a shoe with a larger diameter (100 m), see Figure 10b. The diameter of this shoe is adjusted to ensure a straight configuration of the pipe when it is unloaded, see Figure 10c. The crack on the tension side from the last bending was then examined with silicon replica. This bending and straightening procedure was then repeated to simulate two bending and straightening cycles of the pipes. Pre-straining was performed on two of the three pipes. The pre-straining is not exactly the same as for reel-lay installation. During reel-lay there is a back tension on the pipe and the two straining cycles are not the same, see Figure 2. The pre-straining is, however, assumed to introduce a plastic deformation in the area of the cracks that is relevant for the purpose of the tests.

4 Point Bend Test And Ageing Of Full Scale Pipes

The second part of the testing was performed in a 4 point bend test rig at SINTEF. The pipes were pressurized to 325 bar and tested in bending until failure. In total, three pipes were tested. The pipe that had not undergone pre-straining was tested to serve as a reference point. The pre-strained pipes were tested so that the bending strain capacity was measured on the side that started in tension during pre-straining (12 o'clock) for one pipe, and on the side that started in compression during pre-straining (6 o'clock) for the other pipe.

The test setup used by Østby and Hellesvik [16] was applied. A sketch of the test rig can be seen in Figure 4. The test rig was oriented horizontally. The load was introduced using a 1500 kN hydraulic cylinder. The maximum stroke of the cylinder was 1500 mm. The load from the cylinder was transferred to the inner tension rods through a pair of load spreader plates. The distance between the inner tension rods was 2400 mm, and the distance between the attachment points on the pipe for the outer tension rods was 5500 mm. The end of the outer tension rods represented the fixed points during the tests. To avoid local collapse at the points of introduction of the load in the pipe, the area between the inner and outer tension rods was filled with concrete. The space between the concrete fillings was 1900 mm. A biaxial state of stress was obtained by filling the central portion of the pipes with pressurized water.

Instrumentation and measurements during testing:

- The displacements were measured with displacements transducers at the centre of the pipe and at 2 OD to each side of the center of the pipe.
- The force in the cylinder was measured using the hydraulic pressure.
- The internal pressure was measured using a pressure transducer mounted in one of the end caps of the pipe.
- The Crack Mouth Opening Displacement (CMOD) of the defect was obtained using clip gauges attached to a spark eroded groove in the pipe. The clip gauge was located at the centre of the defect.
- To measure the Crack Tip Opening Displacement (CTOD) and crack growth during the testing, silicone replicas of the defects were made for the initial unloaded crack and at different levels of applied load.

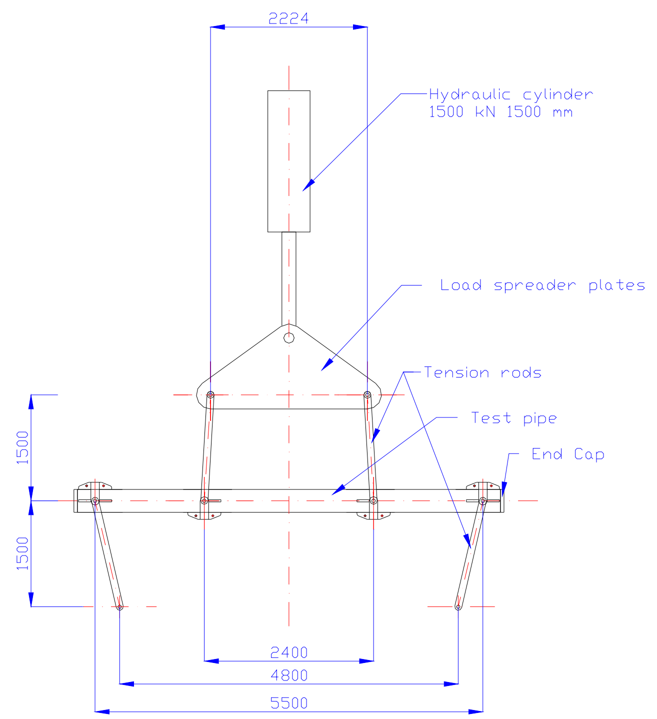

Figure 4 Sketch of the test rig.

RESULTS

Tensile Properties

Tensile testing was performed on pre-strained and unstrained material. The pre-straining was similar to the pre-straining cycles of the pipes at 6 and 12 o'clock. The pre-strained material was artificially aged at 250°C for one hour in accordance to DNV OS-F101 [15]. Tensile specimens were extracted from the prestrained and unstrained material and tested at room temperature. The results are given in Table 1 and Figure 5.

Table 1 Tensile properties for unstrained and pre-strained material. 12 o'clock material ends in compression and 6 o'clock ends in tension from the pre-straining.

I.D.	R_{p02} [MPa]	R_{t05} [MPa]	R_m [MPa]	A_{gt} [%]	R_{p02}/R_m
Unstrained	467	465	565	11.75	0.83
12 o'clock	483	487	568	8.92	0.85
6 o'clock	562	562	591	7.48	0.95

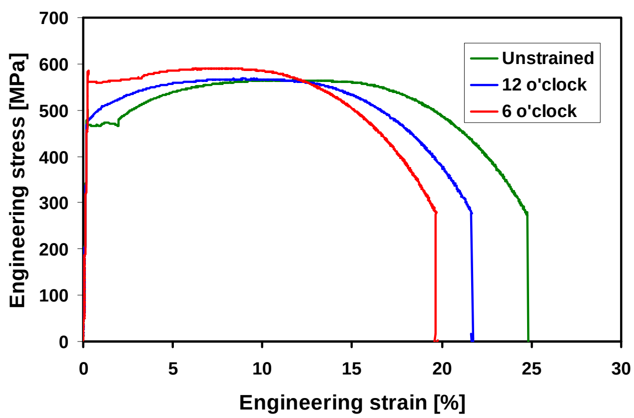

Figure 5 Engineering stress strain curves

There is a significant increase in the yield stress for the 6 o'clock pre-straining. This is due to strain hardening and because the upper and lower yield plateaus are restored after ageing. It is well known that the upper and lower yield plateaus are restored when a material is strained in one direction, aged and strained again in the same direction. If the straining direction is changed the upper and lower yield plateaus are not restored [17, 18]. This is also the reason why there are no upper and lower yield plateaus for the 12 o'clock pre-strained material. The pre-straining for this material ends in compression before it is aged and tested in tension. For the 12 o'clock material there is a normal Bauschinger effect, but the Bauschinger stress-strain curve rises without discontinuity above the former yield level due to hardening from the pre-straining cycles [17].

Fracture Mechanics Testing

The fracture mechanics testing was performed using SENT specimens in accordance to DNV RP-F108 [1]. The material was pre-strained and aged with the same procedure as for the tensile specimens before the crack was introduced to the specimens. The testing was performed at room temperature. All specimens showed a ductile behaviour and the specimens were unloaded at different CTOD to establish R-curves. Geometry, CTOD and ductile crack growth for all specimens are given in Table 2-Table 4. The R-curves are given in Figure 6. The three R-curves are very similar, only small tendencies towards a lower curve for the 12 o'clock material and some more reductions for the 6 o'clock material. The differences are, however, too small to conclude that there is an effect of the pre-straining and ageing process.

Table 2 Results from testing of unstrained SENT specimens

Specimen I.D.	Geometry			At unloading	
	W [mm]	B [mm]	a_0 [mm]	Δa [mm]	CTOD [mm]
S1	15.97	31.85	5.42	1.66	2.58
S2	15.97	31.88	5.59	1.18	2.07
S3	15.98	31.85	5.43	0.86	1.62
S4	15.97	31.86	5.42	0.56	1.21
S5	15.98	31.85	5.63	0.31	0.79
S6	15.96	31.87	5.45	0.13	0.37

Table 3 Results from testing of 12 o'clock material with SENT specimens

Specimen I.D.	Geometry			At unloading	
	W [mm]	B [mm]	a_0 [mm]	Δa [mm]	CTOD [mm]
PS3	16.10	32.04	5.54	1.83	2.54
PS5	16.06	32.04	5.48	1.22	2.03
PS8	16.07	32.09	5.77	0.85	1.56
PS10	16.09	32.03	5.49	0.56	1.13
PS13	16.06	32.04	5.39	0.29	0.73
PS15	16.01	32.06	5.50	0.11	0.33

Table 4 Results from testing of 6 o'clock material with SENT specimens

Specimen I.D.	Geometry			At unloading	
	W [mm]	B [mm]	a_0 [mm]	Δa [mm]	CTOD [mm]
PS14	16.03	31.97	5.44	1.92	2.69
PS2	16.01	32.02	5.29	1.49	2.18
PS4	16.00	31.99	5.41	1.01	1.67
PS7	16.10	31.99	5.42	0.60	1.22
PS9	16.10	32.00	5.38	0.37	0.79
PS12	16.07	32.02	5.65	0.12	0.34

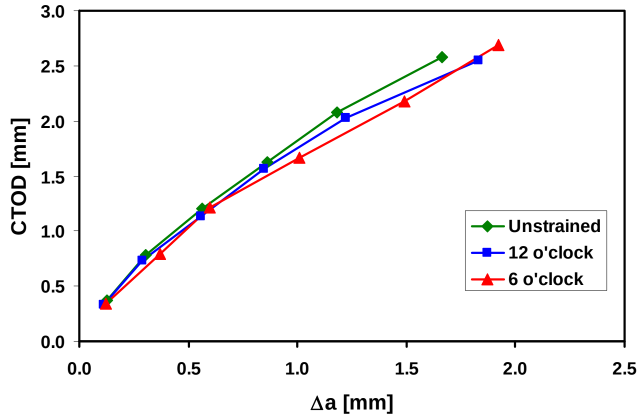

Figure 6 SENT R-curves for unstrained, 12 and 6 o'clock material

Pre-straining And Ageing Of Full Scale Pipes

Unlike small scale testing, the crack for the full scale testing was introduced before pre-straining. Silicon replica during and after pre-straining (previously described reeling simulations) revealed that there was no crack growth during the pre-straining. After pre-straining the pipes were aged for one hour at 250°C.

Four Point Bend Testing Of Full Scale Pipes

Figure 7 shows load versus bending strain for the three full scale tests. The bending strain capacity of the pipe without pre-straining was 5.7%. The pipe that has the 12 o'clock material on the tension side has a bending strain capacity of 2.6 %, and the third pipe with the 6 o'clock material on the tension side has a strain capacity of 1.7%. Silicon replica to establish the CTOD and crack growth was taken at 8 different CMOD levels. Due to safety regulations, the pipes were unloaded during these measurements, as apparent in Figure 7.

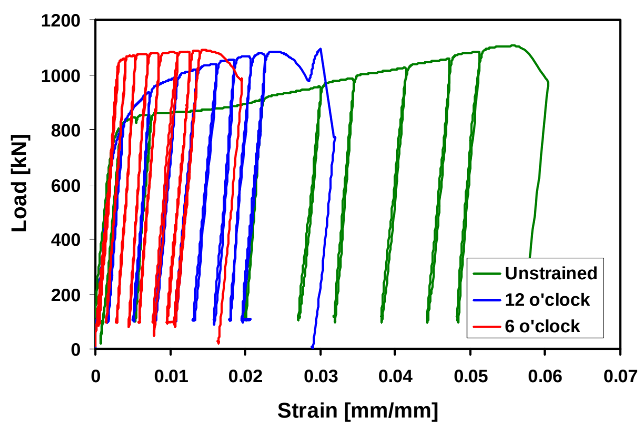

Figure 7 Load versus strain from pipe tests

The curvature was estimated based on the displacement measurements performed on the pipe. The bending strain was calculated according to the following formula:

$$\varepsilon = \frac{r}{R} \tag{1}$$

where r is the outer radius of the pipe, and R is the radius of curvature. This method for calculating the strain was chosen based on experience from Østby and Hellesvik [16]. They used the same test setup and got similar strain obtained using the curvature measurements and strain established from strain gauges.

The differences in load versus strain curves in Figure 7 can be explained by the differences in tensile properties on the tension side of the pipe, see Figure 5. The tensile tests in Figure 5 show that the pre-strained 6 o'clock material has a high yield stress and low hardening. The pre-strained 12 o'clock material has similar yield stress as the unstrained material, but the hardening exponent is much higher. Exactly the same behaviour is seen for the full scale tests, Figure 7. A relation between the CMOD and CTOD was established based on the ratio between the CTOD from the silicon replica and the measured CMOD at each unloading.

From the CTOD versus strain curves in Figure 8, it is seen that the pre-strained pipe with 6 o'clock material on the tension side has the highest driving force for crack growth (CTOD) at all strain levels. The pre-strained pipe with 12 o'clock material on the tension side is in the middle, while the lowest crack driving force is observed for the pipe without pre-straining.

Differences in crack driving force caused by changes in the tensile properties during pre-straining are probably the main reason for the differences in bending strain capacity. However, changes in the R-curves due to pre-straining do also probably play a role.

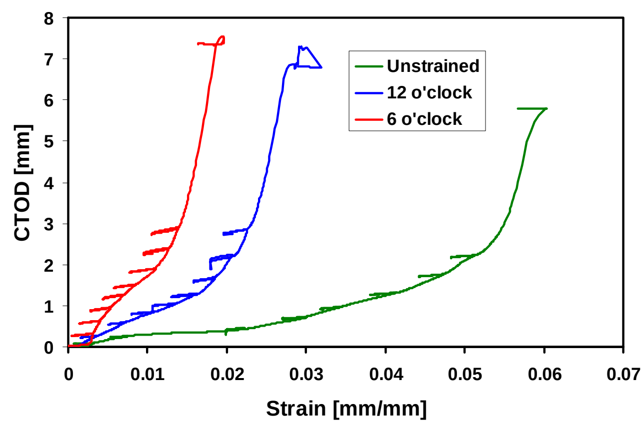

Figure 8 CTOD versus strain from pipe tests

Photos of the pipe deformation at failure are given in Figure 11. Failure is caused by fracture occurring on the tension side as the defect extends through the wall thickness.

The water jet coming out from the pressurized pipes at failure can be seen in the pictures.

Figure 9 shows the R-curves (CTOD versus crack growth) established from the silicon replica. The lowest R-curve is for the pre-strained pipe with 6 o'clock material on the tension side, the pipe with pre-strained 12 o'clock material on the tension side has somewhat higher R-curve and the pipe without pre-straining has the highest R-curve. This is the same ranking as the strain capacity. For the fracture mechanics testing with SENT specimens, in which the effect of pre-straining was insignificant,,the crack was introduced after pre-straining. The results support the findings from Eikrem et al. [5] that there will be accumulated ductile damage from the first load cycle in front of the crack tip, which will reduce the R-curve in the next cycle. The R-curve from the SENT specimen without pre-straining is lower than the R-curve from the pipe without pre-straining. Since this can not be explained by pre-straining, the difference must be caused by differences in the test method. The SENT specimens are designed to have somewhat higher geometry constraint than circumferential surface flaws in pipes to ensure conservative R-curves when used in ECA analyses [19, 20]. This might explain the difference, but differences in the sharpness of the crack tip might also be of influence. The SENT specimens were tested with fatigue sharpened cracks, while the cracks in the pipes were only spark eroded. The experience is, however, that this difference has insignificant influence for ductile materials. Even if the SENT testing is conservative for similar material conditions (unstrained material), the R-curve for the pipe with 6 o'clock material on the tension side has a lower R-curve than the SENT specimen when the material is pre-strained before the notch is introduced.

The results indicate that the procedures for fracture mechanics testing and ECA in DNV-RP-F108 [1] and DNV-OS-F101[15] can be non-conservative.

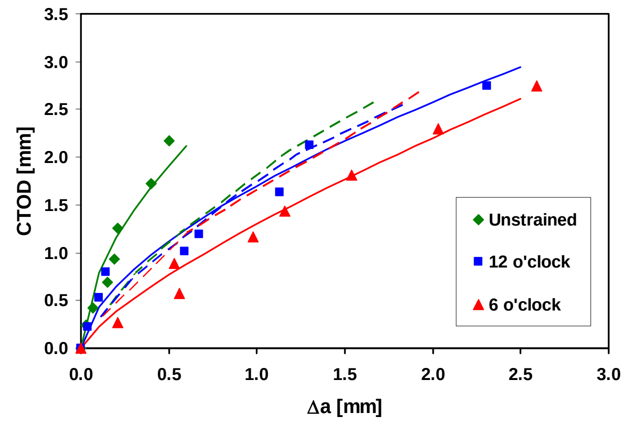

Figure 9 R-curves established from silicon replica of the pipes, R-curves from SENT testing (Figure 6) is given for comparison as dotted lines

The prestraining will introduce residual stresses into the material. On the 6 o'clock side there will be residual stresses in compression, and on the 12 o'clock side there will be residual stresses in tension. It can not be ignored that these residual stresses also play a role for both the driving force and the R-curve [21, 22]. The effect of residual stresses is, however, reduced under high plastic deformation. Since all pipes failed after significant plastic deformation, it is believed that the effect of residual stresses is small compared to the effect of strain ageing and accumulated damage in front of the crack tip.

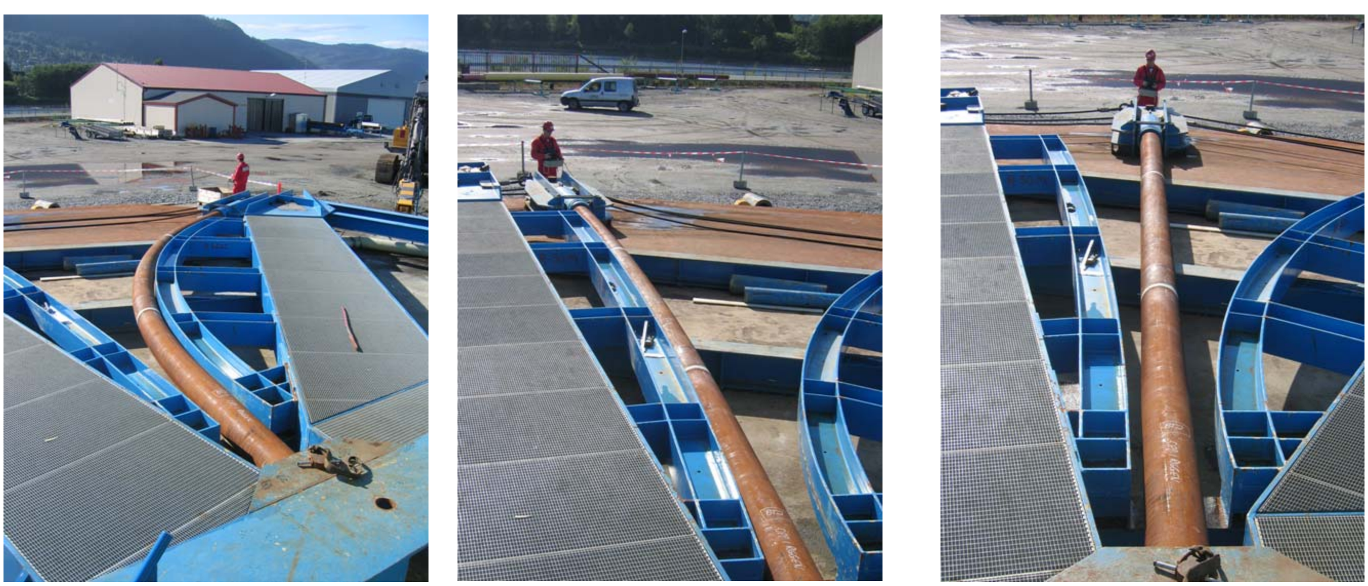

Figure 10 Pre-straining of pipes: a) "reeling on" b) straightening c) unloaded straight pipe

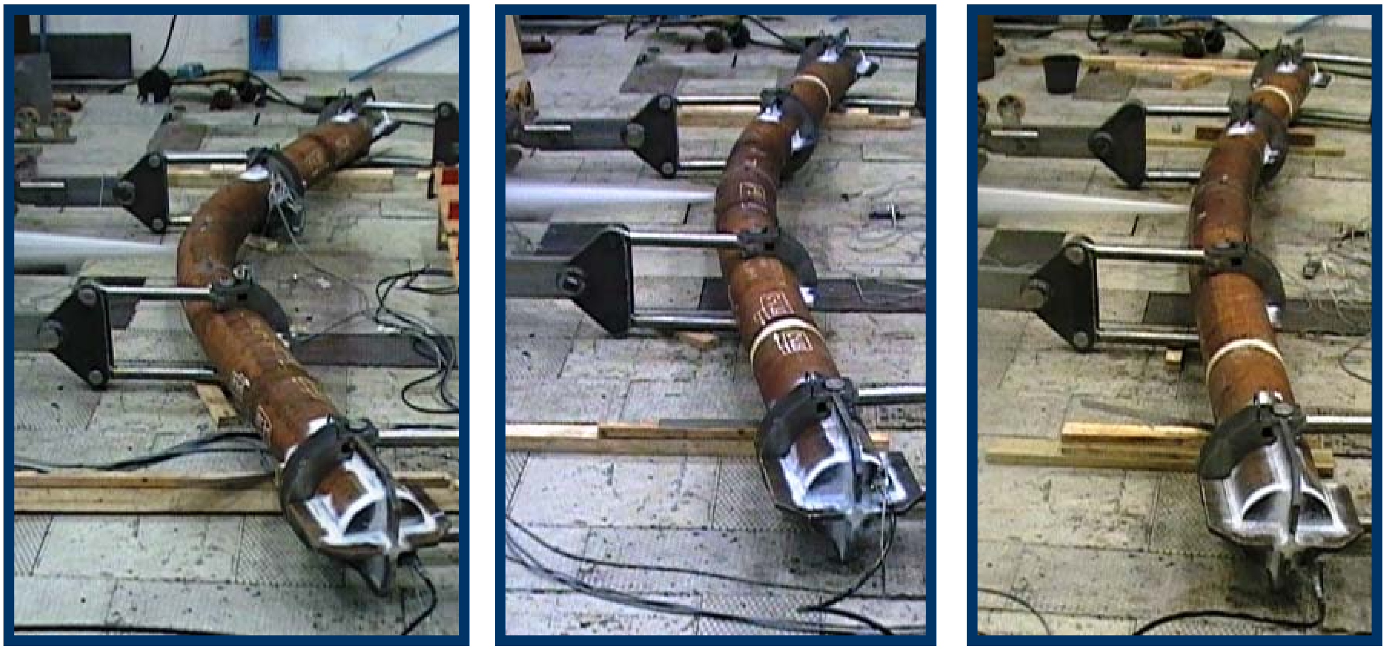

Figure 11 Picture of the pipes at failure, see water jet: a) unstrained pipe (critical bending strain 5.7%)   b) pre-strained pipe, 12 o'clock (critical bending strain 2.6%)   c) pre-strained pipe, 6 o'clock (critical bending strain 1.7%).

CONCLUSIONS

This paper has presented results from large scale testing of pre-strained pipes. Pre-straining was performed to simulate reel-lay installation of offshore pipelines. After pre-straining and ageing, the pipes were tested in 4-point bending until fracture. The aim was to study how the bending strain capacity during operation is influenced by the reel-lay installation when there are flaws from production that interacts with the history of reeling.

The results show that there is a significant effect of pre-straining and how the bending moment during operation coincides with the orientation during installation. The strain capacity for the side of the pipe that ends in tension (6 o'clock) and the side that ends in compression (12 o'clock) from pre-straining was 1.7% and 2.6 % respectively. The strain capacity of the third test without pre-straining was 5.7%.

The differences are explained by two effects of the pre-straining: increased crack driving force and reduced fracture toughness. The 6 o'clock side of the pipe during pre-straining experiences a significant increase in yield stress due to strain ageing, which gave the highest increase in the crack driving force during operation; and the lowest fracture toughness. The 12 o'clock side of the pipe also experiences that the stress-strain curve is elevated due to strain-ageing, but not the yield stress, which is caused by the Bauschinger effect. Also in this case there is a decrease of fracture toughness compared to the unstrained material, but not as much as for the 6 o'clock material.

It is, however, important to note that the notch size in the full scale tests was larger than what would normally be accepted for reeling, and that the notch was positioned in base material and not in the weld metal, which would be a more realistic position for a notch. The welds are normally overmatched and this might reduce the effect of prestraining.

The R-curves established from the pre-strained pipes were compared to small scale fracture mechanics tests on material with the same pre-straining. For these specimens the crack was introduced after pre-straining, while for the pipes the crack was introduced before the pre-straining. For the small scale fracture mechanics testing tested in accordance with current practice, the effect of the pre-straining was insignificant. This indicates that current practice for fracture mechanics testing might be non-conservative when the fracture toughness is used in ECA analyses for operation. Introduction of cracks before pre-straining of small scale fracture mechanics specimens should be considered.

The results highlight that taking pre-strain effects into account in ECA procedures might be of importance, independent of the chosen installation method. This topic should be further investigated.

ACKNOWLEDGMENTS

The financial support from StatoilHydro and Technip Norge is gratefully acknowledged

REFERENCES

1. DNV Recommended practice DNV-RP-F108 "Fracture Control for Pipeline Installation Methods Introducing Cyclic Plastic Strain – 2006", Det Norske Veritas

2. JIP project: Fracture Control for Pipeline Installation Methods Introducing Cyclic Plastic Strains: Development of Guidelines for Reeling of Pipelines, "Testing of Segment Specimens and Full Scale Pipes", DNV Report 2001-3361., Rev 01 2002-02-15.

3. JIP project: Fracture Control for Pipeline Installation Methods Introducing Cyclic Plastic Strains: Development of Guidelines for Reeling of Pipelines, "Report on Task 2 –Determination of Material Properties and Response to Cyclic Straining. Final Version" TWI Report 12201/2c/01, September 2001.

4. JIP project: Fracture Control for Pipeline Installation Methods Introducing Cyclic Plastic Strains: Development of Guidelines for Reeling of Pipelines, "Report on Task 4 –Segment Testing", TWI Report 12201/4/02, July 2002.

5. P. A. Eikrem, Z. L. Zhang and B. Nyhus, Effect of plastic pre-strain on the crack tip constraint of pipeline steels, Int. J of Pressure Vessels and Pipings V84 (2007) p.708.

6. Martinez M. and Brown G., Evolution of pipe properties during reel-lay process: experimental characterisation and finite element modelling, Proceedings of the 24th International Conference on Offshore Mechanics and Arctic Engineering (OMAE 2005), June 12-17, 2005, Halkidiki, Greece.

7. Fukuda N., Hagiwara N., and Masuda T., Effect of pre-strain on tensile and fracture properties of line pipes, J. Offshore Mech. and Artic Engineering, 127 (2005) 263-268.

8. Enami K., The effects of compressive and tensile pre-strain on ductile fracture initiation in steels, Engineering Fracture Mechanics, 72 (2005) 1089-1105.

9. Qiu H., Enoki M., Hiraoka K. and Kishi T., Effect of pre-strain on fracture toughness of ductile structural steels under static and dynamic loading, Engineering Fracture Mechanics, 72 (2005) 1624-1633

10. Cosham A., A Model of Pre-strain Effects on Fracture Toughness, J. Offshore Mech. and Arctic Engineering, 123 (2001) 182-190.

11. Ernst H., Bravo R. E., Daguerre F. and Izquierdo A., Strain history effects on fracture mechanics parameters - application to reeling, Proceedings of the 24th International Conference on Offshore Mechanics and Arctic Engineering (OMAE 2005), June 12-17, 2005, Halkidiki, Greece.

12. Sivaprasad S., Tarafder S., Ranganath V.R. and Ray K.K., Effect of pre-strain on fracture toughness of hsla steels. Materials Science and Engineering, A284 (2000) 195–201.

13. Zhang Z. L., Østby E., Nyhus B. and Ødegård J., Pre-strain history effect on ductile fracture of pipeline steels. In International Seminar on Application of High Strength Line Pipe And Assessment of Pipeline 2006, June, 2006, Xi'an, China.

14. Eikrem P.A., Zhang Z.L. and Nyhus B., Effect of plastic pre-strain on the crack tip constraint of pipeline steels, Int J Pressure Vessels Pipings 2007;84: 708-715.

15. DNV Offshore Standard OS-F101 "Submarine Pipeline Systems – 2007", Det Norske Veritas

16. Østby E, Hellesvik A. "Large scale testing results of the effect of biaxial loading on the deformation capacity of pipes with defects". International Journal of Pressure Vessels and Piping 85, 2008, 814-824

17. Robert A. Elliot, Egon Orowan, Teruyoshi Udoguchi, Ali S. Argon, Absence of yield points in iron on strain reversal after aging, and the Bauschinger overshoot, Mechanics of Materials, Volume 36, Issue 11, November 2004, Pages 1143-1153

18. V. Taupin, S. Varadhan, C. Fressengeas, A.J. Beaudoin, Directionality of yield point in strain-aged steels: The role of polar dislocations, Acta Materialia, Volume 56, Issue 13, August 2008, Pages 3002-3010

19. Nyhus, B., Loria, M. P. and Ørjasæter, O. L., "SENT specimens an alternative to SENB specimens for fracture mechanics testing of pipelines", Proceedings of OMAE03, 22ND International Conference on Offshore Mechanics and Arctic Engineering, June 8–13, 2003, Cancun, Mexico

20. Nyhus B, Østby, E, Knagenhjelm HO, Black S, Røstadsand (2005)."Fracture Control-Offshore Pipelines – Experimental studies on the effect of crack depth and asymmetric geometries on the ductile tearing resistance". Proceeding of OMAE2005, 24th International Conference on Offshore Mechanics and Arctic Engineering, June 12-17, Halkidiki, GreecPut references here.

21. J. Liu, Z. L. Zhang and B. Nyhus, Residual stress induced crack tip constraint, *Engineering Fracture Mechanics*, **75**(2008):4151-4166

22. X. B. Ren, Z. L. Zhang and B. Nyhus, Residual stress induced crack-tip constraint: A parameter study, 17th European Conference on Fracture, 2-4 September, 2008, Brno, Czech Republic.

